

Absolute distance measurement using wavelength-multiplexed phase-locked laser diode interferometry

Takamasa Suzuki, MEMBER SPIE
Osami Sasaki
Takeo Maruyama
Niigata University
Faculty of Engineering
8050 Ikarashi 2 Niigata 950-21
Japan

Abstract. A new type of two-wavelength interferometer which applies a phase-lock technique is described. The wavelength tunability of a laser diode (LD) is used for phase modulation and phase control in this interferometer. Since the two wavelengths are derived from a single LD in our system, the optical system is simple and there is no need to consider the fluctuation of relative wavelength between the two LD's in the conventional two-wavelength interferometers. The equivalent wavelength Λ is 15 mm and the measurement accuracy reaches $\sim\Lambda/400$. The error sources in the system and the error analysis are also described.
© 1996 Society of Photo-Optical Instrumentation Engineers.

Subject terms: two-wavelength interferometers; laser diodes; phase lock.

Paper 34035 received Mar. 25, 1995; revised manuscript received June 23, 1995; accepted for publication June 24, 1995.

1 Introduction

Optical interferometers have been widely used in precise manufacturing or optical testing because they are simple in construction and accurate in measurement in a noncontact way. However, the measured phase is relative and it is limited to less than a half wavelength in distance with one-color interferometers, so phase unwrapping must be performed for measurements of relatively long distance. Moreover, when the step heights on the surface of the object are larger than a half wavelength, exact profilometry cannot be carried out because ambiguities of an integer that is a multiple of 2π occur in the optical phase difference.

On the other hand, it is well known that absolute distance measurement can be achieved by using two different wavelengths. There are many kinds of two-wavelength interferometers (TWIs) such as two-wavelength holographic interferometry,¹ two-wavelength phase shifting interferometry,^{2,3} and two-wavelength heterodyne speckle interferometry.⁴

Nowadays, since various wavelengths between the visible and infrared are available in laser diodes (LD), they are often used in TWIs.^{5–8} They first detect the phase of the test surface for each wavelength. The distance to the test surface is obtained by detecting the difference of the two phases obtained. In this type of TWI, it is difficult to align the optical axes for each LD. Moreover, when two LDs are driven independently, it is important to control the relative change of the wavelengths to stabilize the synthetic wavelength, as pointed out in Ref. 8. The stabilization of the relative change of the wavelengths becomes more important as the difference of the two wavelengths gets smaller.

If a single light source is used, however, there is no need to consider the above problem. A TWI using a single LD has been proposed⁹ in which the temporally multiplexed wavelengths were generated with a rectangular modulation current and the phase was detected by the heterodyne

method using an acousto-optic Bragg cell. In this type of interferometer, there is no need to align the optical axes. Also, the stabilization of the synthetic wavelength is not required because the relative change of the wavelength is constant in the single LD. The synthetic wavelength depends on only the amplitude of the rectangular injection current.

In this paper, we propose a new TWI using a single LD. Consequently, the wavelength is temporally multiplexed, but the approach for the distance measurement is different from that in Ref. 9. Since the difference of the two wavelengths derived from a single LD is very slight in this kind of TWI, the equivalent wavelength then becomes very large and a large measurement range is obtained. However, it is difficult to measure the distance with a high accuracy because of the large equivalent wavelength. So we have applied phase-locked laser diode (PLLD) interferometry^{10,11} to detect the distance accurately. In our system, the phase determined by the optical path difference is temporally controlled to two different constant values by the differential type of PLLD interferometry.¹² The distance is calculated from the difference of the temporally multiplexed injection currents required for the phase control.

In Sec. 2, we describe the principle of the absolute distance measurement. In Sec. 3 and Sec. 4, we give an error analysis and experimental results, respectively.

2 Principle

The experimental setup of the wavelength-multiplexed PLLD interferometer is shown in Fig. 1. The light from the LD is collimated with a lens L and is led to the Twyman-Green interferometer whose optical path difference is $2D_0$. The reference beam and the object beam are reflected by mirrors $M1$ and $M2$, respectively. They are interfered on the charge coupled device (CCD) image sensor and the

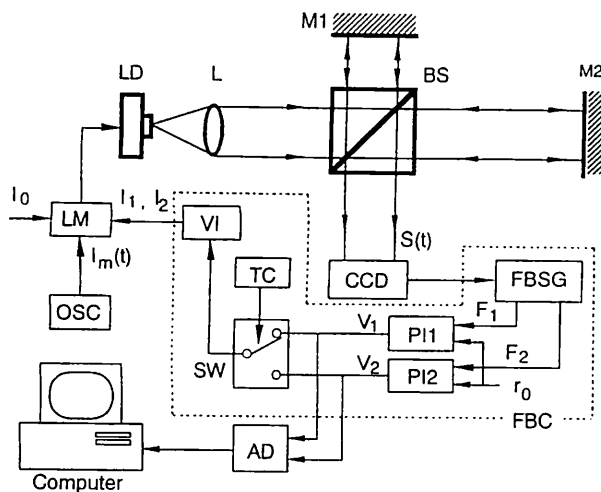


Fig. 1 Experimental setup of a wavelength-multiplexed phase-locked laser diode interferometer. A laser diode (LD) is modulated by using the laser diode modulator (LM). The light is collimated by a lens (L) and led to the Twyman-Green interferometer which consists of mirrors M1 and M2, and a beam splitter (BS). The interference signal $S(t)$ is detected by a CCD image sensor and the wavelength of LD is controlled by a feedback controller (FBC). The FBC consists of a feedback signal generator (FBSG), two PI controllers PI1 and PI2, a timing controller (TC), a switch (SW), and a voltage-to-current converter (VI).

interference signal $S(t)$ is obtained. We used the CCD image sensor as a photodetector to generate the feedback signals as quickly as possible.¹¹

The injection current of the LD consists of a dc bias current I_0 , a sinusoidal modulating current

$$I_m(t) = a \cos(\omega_c t + \theta), \quad (1)$$

and a control current I_1 or I_2 generated by the feedback controller (FBC). The central wavelength λ_0 is determined by I_0 and the wavelength is changed with I_1 , I_2 , and $I_m(t)$ by βI_1 , βI_2 , and $\beta I_m(t)$, respectively, where β is the modulation efficiency of the LD. If the control current is zero, the interference signal $S(t)$ is given by¹⁰

$$S(t) = S_1 + S_0 \cos[z \cos(\omega_c t + \theta) + \alpha], \quad (2)$$

where $z = 4\pi a \beta D_0 / \lambda_0^2$,

$$\alpha = 4\pi D_0 / \lambda_0, \quad (3)$$

S_1 is a dc component, and S_0 is the amplitude of the ac component of $S(t)$.

If the wavelength of the LD is controlled to λ_1 and λ_2 alternately, the corresponding phases α_1 and α_2 are represented by

$$\alpha_1 = 4\pi D_0 / \lambda_1, \quad (4)$$

and

$$\alpha_2 = 4\pi D_0 / \lambda_2. \quad (5)$$

The difference of α_1 and α_2 is calculated as

$$\Delta \alpha = \alpha_2 - \alpha_1 = 4\pi D_0 / \Lambda, \quad (6)$$

where

$$\Lambda = \lambda_1 \lambda_2 / (\lambda_1 - \lambda_2) \quad (7)$$

is an equivalent wavelength. The Λ is larger than the optical wavelength and becomes larger as the difference between λ_1 and λ_2 gets smaller. From Eq. (6), the absolute distance D_0 is given by

$$D_0 = \frac{\Lambda}{4\pi} \Delta \alpha. \quad (8)$$

That is, D_0 can be obtained if the equivalent wavelength Λ and the phase difference $\Delta \alpha$ are known.

The FBC consists of the feedback signal generator (FBSG), two proportional-integral (PI) controllers PI1 and PI2, switch (SW), timing controller (TC), and voltage-to-current converter (VI) whose gain is K_V . The SW alternately changes the control voltage generated by the PI controllers. The timing of the switchover is determined by the TC.

The output signal of the CCD image sensor is obtained as¹³

$$p_i = \int_{(T/4)(i-1)}^{(T/4)i} S(t) dt, \quad (9)$$

where $T = 2\pi/\omega_c$ is the period of the modulation current. Executing additions and subtractions by using p_i , we can quickly obtain the feedback signals

$$F_S(\alpha) = p_1 + p_2 - p_3 - p_4 = A_s \sin \alpha, \quad (10)$$

and

$$F_C(\alpha) = p_1 - p_2 + p_3 - p_4 = A_c \cos \alpha, \quad (11)$$

where A_s and A_c are the functions of z and θ . They are given by¹⁴

$$A_s = (4S_0 T / \pi) \sum_{n=1}^{\infty} [J_{2n-1}(z)/(2n-1)](-1)^n \times \sin[(2n-1)\theta], \quad (12)$$

$$A_c = (4S_0 T / \pi) \sum_{n=1}^{\infty} [J_{2n}(z)/2n][1 - (-1)^n] \times \sin(2n\theta), \quad (13)$$

and $J_n(z)$ is an n 'th-order Bessel function.

Now suppose that $F_s(\alpha)$ or $F_c(\alpha)$ is used as a feedback signal $F(\alpha)$. Inverting $F(\alpha)$, we obtain another feedback signal $-F(\alpha)$, which is lagged by π against $F(\alpha)$. The feedback signals are illustrated in Fig. 2. Each feedback signal is fed to the PI controller and phase lock is carried out, where V_1 and V_2 , the outputs of PI1 and PI2, are temporally multiplexed by the SW and TC. If the reference signal r_0 is set to zero, the feedback circuits move the initial phases α_0 to each of the stable points P_1 and P_2 by

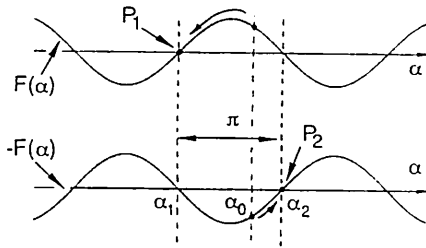


Fig. 2 Illustration of the principle of phase-locked interferometry. The initial phase α_0 s are controlled to each stable phase α_1 and α_2 , which are indicated on the feedback signals $F(\alpha)$ and $-F(\alpha)$ as points P_1 and P_2 , respectively. The phase difference between P_1 and P_2 becomes π accurately.

changing the wavelength of the LD. The phases at the stable point are $\alpha_1=2n\pi$, and $\alpha_2=(2n+1)\pi$, respectively, because the feedback gains are positive and the feedback loop is stable at those points. Consequently, the phase difference $\Delta\alpha$ becomes π accurately and the absolute distance D_0 is given by

$$D_0 = \frac{\Lambda}{4}. \quad (14)$$

Equation (14) shows that the absolute distance is derived from the equivalent wavelength. The wavelengths for α_1 and α_2 are then represented by

$$\lambda_1 = \lambda_0 + \beta I_1 = \lambda_0 + \beta K_V V_1, \quad (15)$$

$$\lambda_2 = \lambda_0 + \beta I_2 = \lambda_0 + \beta K_V V_2, \quad (16)$$

respectively, where I_1 and I_2 are the control currents required for the phase lock.

From Eqs. (7), (15), and (16), the equivalent wavelength Λ is calculated as

$$\Lambda = \frac{\lambda_0^2}{\beta K_V (V_1 - V_2)}, \quad (17)$$

where the conditions of $\lambda_0 \gg \beta K_V V_1$, $\lambda_0 \gg \beta K_V V_2$ are used. From Eqs. (14) and (17), the absolute distance D_0 is given by

$$D_0 = \frac{C}{\Delta V}, \quad (18)$$

where $C = \lambda_0^2 / 4\beta K_V$ is a constant and $\Delta V = V_1 - V_2$ is the difference of the control voltages. The absolute distance can be obtained by measuring V_1 and V_2 , the outputs of the two PI controllers. The control voltages V_1 and V_2 are sampled by the analog-to-digital (A/D) converter (AD) and D_0 is calculated from Eq. (18) by using a computer.

3 Error Analysis

Generally the measurement error in interferometers is mainly due to external disturbances. However, when the external disturbance is comparatively small, the phase error is compensated¹² with differential detection in the differential type of PLLD interferometer. The other expected error

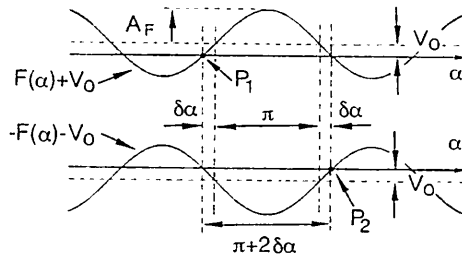


Fig. 3 Illustration of the feedback signals which contain the offset voltage V_0 . The phase difference between P_1 and P_2 becomes larger than π .

sources are the electrical noise, the error in the amplitude a and phase θ of the modulating current, amplitude modulation introduced by the direct modulation, and the quantizing error in the A/D converter. However, the electrical noise and the errors in the modulating current can be removed easily by adjusting the electrical circuits. Here we investigate the influence of the amplitude modulation of the light caused by the sinusoidal phase-modulating current injected into the LD and next the measurement error caused by the quantizing error in the A/D converter.

When the injection current of the LD is modulated, the output beam of the LD is changed not only in phase but also in intensity. If the modulation signal is a sinusoid as shown in Eq. (1), the intensity-modulated interference signal is represented by

$$S_I(t) = [1 + a \gamma \cos(\omega_C t + \theta)] S(t), \quad (19)$$

where a is an amplitude of $I_m(t)$ and γ is an intensity modulation efficiency of LD. Inserting Eq. (19) into Eq. (9) and calculating F_C and F_S by using Eqs. (10) and (11), an offset component

$$V_O = (-4a \gamma S_1 / \omega_C) \sin \theta \quad (20)$$

is derived only in F_S while the offset component in F_C is zero. When the feedback signal contains an offset component as shown in Fig. 3, the phase difference $\Delta\alpha$ becomes $\pi+2\delta\alpha$. When the amplitude of $F(\alpha)$ is A_F , the phase error $2\delta\alpha$ is given by

$$2\delta\alpha = 2 \sin^{-1}(V_O / A_F), \quad (21)$$

and the measured distance is given by

$$D_0' = \frac{\Lambda}{4} (\pi + 2\delta\alpha) = \frac{\Lambda}{4} + \delta D_1, \quad (22)$$

where $\delta D_1 = (\Lambda/2\pi)\delta\alpha$ is a measurement error caused by the offset voltage. It is a fatal measurement error because the equivalent wavelength Λ is very large in this interferometer. To remove this fatal error, we used $F_C(\alpha)$ as a feedback signal.

Next, we analyze the influence of the quantizing error of the A/D converter. Supposing that the bit number and the maximum input voltage of the A/D converter are N and $\pm V_m$, respectively, the quantizing error becomes

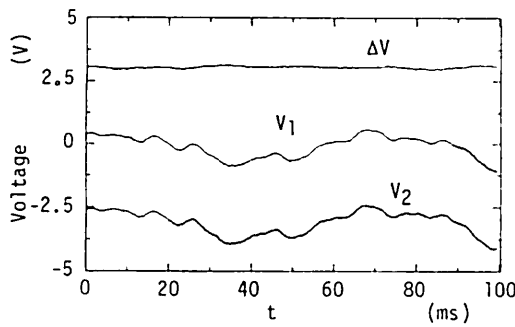


Fig. 4 The evolutions of the control voltage V_1 and V_2 , and the differential voltage ΔV .

$$\delta V = 2V_m/2^N. \quad (23)$$

Then the measured distance is given by

$$D_0'' = \frac{C}{\Delta V + \delta V} \approx \frac{C}{\Delta V} + \delta D_2, \quad (24)$$

where $\delta D_2 = -D_0 \delta V / \Delta V$ is a measurement error in distance caused by the quantizing error in the A/D converter.

4 Experimental Results

The experimental setup is shown in Fig. 1. The light source was an AlGaAs laser diode (Hitachi HL7801) whose maximum power was 5 mW and central wavelength λ_0 was 780 nm. The modulation efficiency β was 6.8×10^{-3} nm/mA. The readout frequency of the CCD image sensor was 2 MHz. The modulation frequency $2\pi/\omega_C = 1/T$ was set to 2 kHz. The timing controller (TC) alternately changed the SW every 20 periods of the modulation current. That is, the SW changed every 10 ms. The gain K_V of the VI is 1.7×10^{-1} mA/V. The bit number and the maximum input voltage of the A/D converter are $N=12$ and $V_m = \pm 10$ V, respectively. The modulation amplitude z and initial phase θ were set to the optimum values,¹³ 2.45 and -56 deg.

The evolution of the control voltages V_1 and V_2 , and the differential voltage $\Delta V = V_1 - V_2$ at $D_0 \sim 44$ mm is shown in Fig. 4. In this case, the equivalent wavelength is calculated as $\Lambda = 4D_0 \sim 176$ mm by using Eq. (18). The control voltages are changed temporally by the external disturbances, but the changes are the same. So the influence of the external disturbance is almost removed by the differential detection, and the differential voltage becomes constant.

The differential voltage ΔV versus distance D_0 is calculated in Fig. 5 by using Eq. (18) and the constants in the experimental setup. Obviously, from Eq. (24), the measurement error caused by the A/D converter becomes smaller as $D_0/\Delta V$ becomes smaller, so that the ΔV must be selected as large as possible. Considering $|V_m| < 10$ V, we set $D_0 \sim 15$ mm in the following experiment. Consequently, the ΔV and the equivalent wavelength Λ become ~ 8.77 V and ~ 60 mm, respectively. The conversion error δV in the A/D converter is 4.88 mV and the measurement error in distance becomes 8.35×10^{-3} mm.

Next, we measured the amplitude and the offset voltage of the feedback signals F_C and F_S with changing the dc

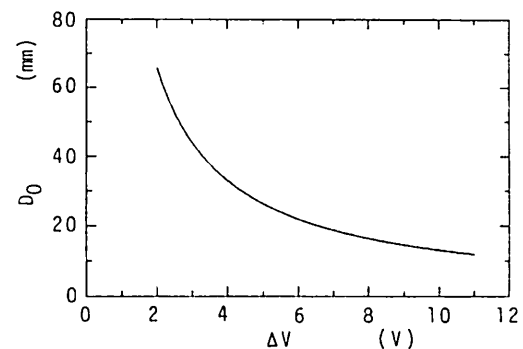


Fig. 5 The relation between differential voltage ΔV and the measured distance D_0 at the experimental constants.

bias current I_0 , where a , the amplitude of the modulation current, was constant to keep $z=2.45$. The amplitudes of the feedback signal are shown in Fig. 6. They are measured by changing the phase α with a sinusoidally vibrated piezoelectric transducer mounted on the object mirror M2. They increase as the dc bias current I_0 increases, because S_0 , the amplitude of the ac component, increases with I_0 in Eqs. (12) and (13). It was confirmed that the feedback signals are not saturated when I_0 is changed from 50 to 58 mA.

The offset voltages of the feedback signals are shown in Fig. 7. In F_C , the offset was not detected while I_0 was relatively small but a little offset was detected when I_0 was greater than 53.2 mA. The amplitude A_F and the maximum offset of F_C was ~ 2.7 V and ~ 0.025 V, respectively, at $I_0=55.6$ mA. Consequently, the phase error $\delta\alpha$ is calculated as 9.3×10^{-3} rad, which is equivalent to a measurement error of 0.044 mm. On the other hand, in F_S , the offset was ~ 0.23 V at $I_0=55.6$ mA and this is equivalent to a measurement error of 0.36 mm. Figure 7 shows that the offset voltage in the feedback signal F_S is increased with I_0 , which increases the dc component S_1 in Eq. (20), while the offset voltage in F_C is scarcely increased. It is thought that the offset voltage detected in F_C is the total offset

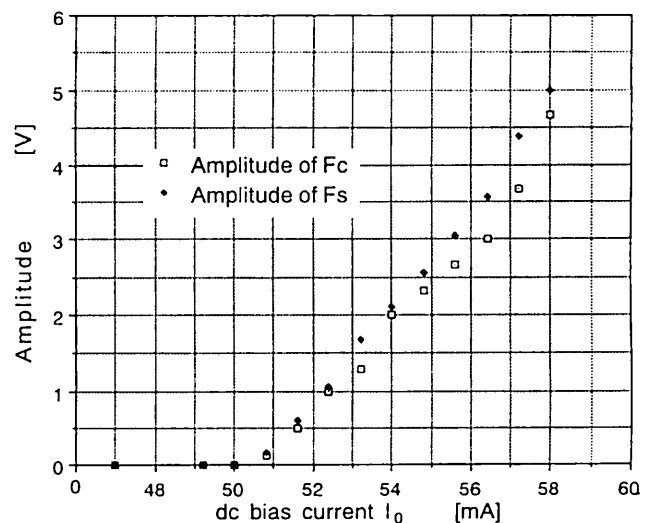


Fig. 6 Amplitude of the feedback signals measured with the change of the dc bias current of LD.

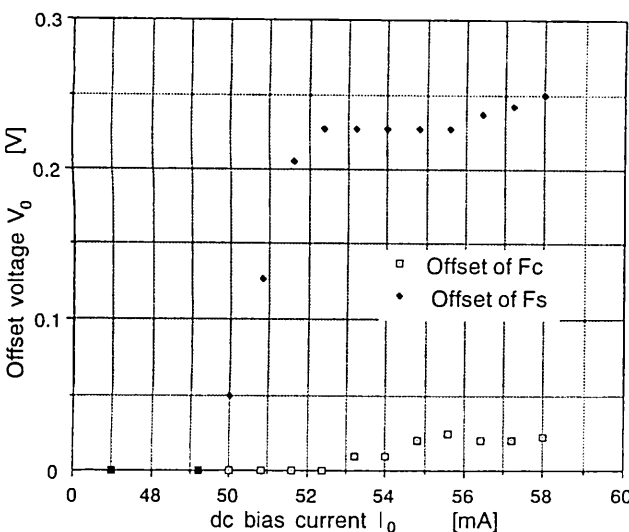


Fig. 7 Offset voltages of the feedback signals measured with the change of the dc bias current of LD.

voltage of the electric devices in the FBSG and PI controller. The generation of the offset voltage in F_S , discussed in Sec. 3, was confirmed from Fig. 7.

Finally, we measured the displacement of the object mirror M_2 . The mirror was mounted on the $X-Y$ stage and moved from $D_0=15$ mm to 17.5 mm in discrete 0.5-mm increments by using a micrometer. The measurement result is shown in Fig. 8. The measurement values agree well with the theoretical line. The standard deviation was ~ 0.147 mm in this measurement. So the accuracy of this interferometer is experimentally obtained as $\sim \Lambda/400$.

Since the variable range of the control current for LD is generally ~ 10 mA if mode hopping does not occur, the minimum equivalent wavelength Λ becomes ~ 8.95 mm in this type of TWI, which uses only one LD, and the measurable range would be $\Lambda/2\sim 4.5$ mm. When Λ or D_0 gets

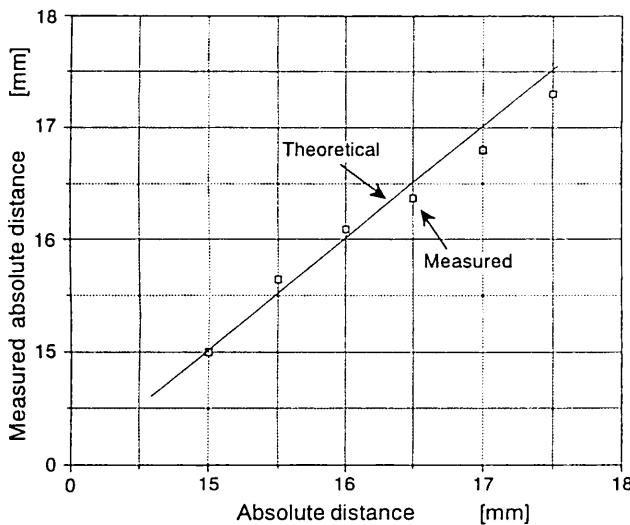


Fig. 8 Measured absolute distance when the object mirror M_2 was moved from 15 to 17.5 mm in discrete 0.5-mm increments. The standard deviation was ~ 0.147 mm in this experiment.

smaller, however, the measurement errors due to the amplitude modulation and the quantizing error in the A/D converter are decreased according to Eqs. (22) and (24). The resolution then would be ~ 20 μ m if the measurement accuracy is maintained at $\Lambda/400$ by using phase-locked interferometry.

5 Conclusions

We have presented the principle, error analysis, and experimental results of a new TWI which uses only one LD. In our system, external disturbances are removed because the differential type of phase-locked interferometry is applied. The distance can be obtained by measuring only the phase-control voltage. That is, there is no need to detect the phase in the interference signal. The error occurs in the A/D converter and the feedback signal generator, but the significant error occurs in the latter. The accuracy can be improved by (1) decreasing the parameter $D_0/\Delta V$, (2) adjusting the offset voltage of the feedback signal, and (3) decreasing the equivalent wavelength. The measurement accuracy is obtained as $\sim \Lambda/400$ experimentally. Since this system uses a CCD image sensor as a photodetector, it is easy to implement an extension to one- or two-dimensional measurements.

Acknowledgment

The authors are grateful to Takefumi Itakura for his help with the experiments. This work was supported by a scientific research grant from the Ministry of Education of Japan, contract no. 05750405.

References

1. J. C. Wyant, "Testing aspherics using two-wavelength holography," *Appl. Opt.* **10**, 2113–2118 (1971).
2. Y.-Y. Cheng and J. C. Wyant, "Two-wavelength phase shifting interferometry," *Appl. Opt.* **23**, 4539–4543 (1984).
3. K. Creath, Y.-Y. Cheng, and J. C. Wyant, "Contouring aspheric surfaces using two-wavelength phase-shifting interferometry," *Opt. Act.* **32**, 1455–1464 (1985).
4. A. F. Fercher, H. Z. Hu, and U. Vry, "Rough surface interferometry with a two-wavelength heterodyne speckle interferometer," *Appl. Opt.* **24**, 2181–2188 (1985).
5. A. J. den Boef, "Two-wavelength scanning spot interferometer using single-frequency diode lasers," *Appl. Opt.* **27**, 306–311 (1988).
6. O. Sasaki, H. Sasazaki, and T. Suzuki, "Two-wavelength sinusoidal phase/modulating laser diode interferometer in sensitive to external disturbances," *Appl. Opt.* **30**, 4040–4045 (1991).
7. Y. Ishii and R. Onodera, "Two-wavelength laser-diode interferometry that uses phase-shifting techniques," *Opt. Lett.* **16**, 1523–1525 (1991).
8. P. de Groot and S. Kishner, "Synthetic wavelength stabilization for two-color laser-diode interferometry," *Appl. Opt.* **30**, 4026–4033 (1991).
9. C. C. Williams and K. Wickramasinghe, "Optical ranging by wavelength multiplexed interferometry," *J. Appl. Phys.* **60**, 1900–1903 (1986).
10. T. Suzuki, O. Sasaki, and T. Maruyama, "Phase locked laser diode interferometry for surface profile measurement," *Appl. Opt.* **28**, 4407–4410 (1989).
11. T. Suzuki, O. Sasaki, K. Higuchi, and T. Maruyama, "Phase-locked laser diode interferometer: high speed feedback system," *Appl. Opt.* **30**, 3622–3626 (1991).
12. T. Suzuki, O. Sasaki, K. Higuchi, and T. Maruyama, "Differential type of phase-locked laser diode interferometer free from external disturbance," *Appl. Opt.* **31**, 7242–7248 (1992).
13. O. Sasaki, H. Okazaki, and M. Sakai, "Sinusoidal phase modulating interferometer using the integrating-bucket method," *Appl. Opt.* **26**, 1089–1093 (1987).
14. T. Suzuki, O. Sasaki, J. Kaneda, and T. Maruyama, "Real-time two-dimensional surface profile measurement in a sinusoidal phase-modulating laser diode interferometer," *Opt. Eng.* **33**, 2754–2759 (1994).



Takamasa Suzuki received a BE in electrical engineering from Niigata University in 1982, a ME degree in electrical engineering from Tohoku University in 1984, and a DrEng in electrical engineering from the Tokyo Institute of Technology in 1994. He is an associate professor of electrical and electronic engineering at Niigata University. Since 1987 he has worked on interferometers using laser diodes and applications of phase conjugate optics at Niigata University.



Takeo Maruyama received a BE degree in electrical engineering from Niigata University in 1965 and a DrEng in electrical engineering from Nagoya University in 1979. He is a professor of electrical and electronic engineering at Niigata University. Since 1965 he has worked in the field of physics of ionized gases and optical metrology.



Osami Sasaki received BE and ME degrees in electrical engineering from Niigata University in 1972 and 1974, respectively, and a DrEng degree in electrical engineering from the Tokyo Institute of Technology in 1981. He is a professor of electrical and electronic engineering at Niigata University. Since 1974 he has worked in the field of optical measuring systems and optical information processing.